

Thermocapillary migration and interactions of two nondeformable droplets

Z. Yin,* L. Chang, W. Hu, and P. Gao
National Microgravity Laboratory, Institute of Mechanics,
Chinese Academy of Sciences, Beijing 100190, P.R.China
(Dated: August 4, 2018)

A numerical study on interactions of two spherical drops in thermocapillary migration in microgravity is presented. Finite-difference methods were adopted and the interfaces of drops were captured by the front-tracking technique. It is found that the arrangement of drops directly influences their migrations and interaction, and that the motion of one drop is mainly determined by the disturbed temperature field because of the existence of the other drop.

PACS numbers: 05.70.Np, 02.70.Bf, 05.70.-a

Introduction

Under the microgravity condition, the thermocapillary migration of droplets or bubbles in matrix liquid is caused by the nonuniform interface tension introduced by the temperature gradient. This motion is of great importance in material processing and other applications in space. The original work in this field was performed by Young *et al.*[1]. In their study, the inertial convection and thermal convection are neglected (the so-called *YGB* Model), and the derived migration velocity is

$$V_{YGB} = \frac{2U}{(2 + 3\mu_d/\mu_b)(2 + k_d/k_b)}. \quad (1)$$

Here, U is the reference velocity defined by the balance of thermocapillary force and viscosity force on the drop/bubble:

$$U = |\sigma_T| |\nabla T_\infty| a / \mu_b,$$

μ is the kinematic viscosity, k the thermal conductivity, σ_T the rate of change of interfacial tension with temperature, ∇T_∞ the temperature gradient imposed on matrix liquid, and a the radius of the drop or bubble. The symbols with the subscript d mean the parameters of the droplet/bubble, and those of the bulk liquid are indicated by the subscript b .

After *YGB*, there are many other studies on the thermocapillary motion of isolated drop/bubble (see [2] and references therein). In practice, it is common to have two or more drops/bubbles in the continues phase, so it is necessary to study their interactions. The first axisymmetric investigation of two thermocapillary bubbles was

conducted by Meyyappan *et al.*[3], using the bipolar coordinate. It was found that the smaller bubble always moves faster than the isolated drop while the bigger one moves slightly slower. Meyyappan and Subramanian[4] extended the above work to arbitrarily placed bubbles. Balasubramanian and Subramanian[5] assumed that two bubbles migrated in the potential flow (namely, the related Re number is very large), and the matched asymptotic analysis was adopted to solve the energy equation with large Ma numbers. It was found that the thermal wake of the leading bubble will disturb the temperature field around the trailing bubble and reduce its velocity. Interactions between two spherical droplets were firstly studied by Anderson with a reflection method[6]. It was found that interactions between droplets driven by thermocapillary effects are much weaker than those of sedimentation. Ken and Chen[7] analyzed the axisymmetric motion of two droplets in the bishperical coordinate, and their later combined analytical-numerical study was about a finite chain of spherical droplets along the line of their centers [8]. Interactions of two deformable droplets in the axisymmetric coordinate were studied by Zhou and Davis[9]. Thermocapillary interactions of droplets or bubbles toward a hot wall at finite Reynolds and Marangoni numbers were numerically studied by Nas *et al.*[10, 11]. It was found that bubbles and light drops line up perpendicular to the temperature gradient and are evenly spaced in the horizontal direction. A space experiment observed that a small leading drop could retard the movement of the big trailing drop [12].

So far as we know, there is no systematic study on the interaction of two arbitrarily placed drops in the thermocapillary research, and it will be the main subject here. We focus our investigation on two droplets with equal size and the same physical parameters (kinematic viscos-

*Electronic address: zhaohua.yin@imech.ac.cn

ity, thermal diffusivity, density, and specific heat). The governing equations and numerical methods will be introduced in the next section, detailed numerical models and parameters of simulations are in section 2, and the results when the inertia and thermal convection are ignorable or not, are discussed in section 3 and 4, respectively.

I. GOVERNING EQUATIONS AND NUMERICAL METHODS

In the thermocapillary motion, the two droplets with the same radius a are surrounded by the bulk fluid in a rectangular box $\Omega = [x_0, x_1] \times [y_0, y_1] \times [z_0, z_1]$ (Fig. 1). The box is closed by no-slip walls. The direction of the temperature gradient is along the z axis, and $x = 0$ is treated in the drop centers. The governing equations for this problem are:

$$\begin{aligned} \nabla \cdot \mathbf{u} &= 0, \\ \frac{\partial(\rho\mathbf{u})}{\partial t} + \nabla \cdot (\rho\mathbf{u}\mathbf{u}) &= -\nabla p + \nabla \cdot (\mu(\nabla\mathbf{u} + \nabla^T\mathbf{u})) + \mathbf{F}_\sigma, \\ \rho C_p \left(\frac{\partial T}{\partial t} + \mathbf{u} \cdot \nabla T \right) &= \nabla \cdot (k\nabla T). \end{aligned}$$

Here, $\mathbf{u} = (u, v, w)$, $\mathbf{x} = (x, y, z) \in \Omega$. \mathbf{F}_σ is the body force term calculated by integrating the surface tension across the interface[2]. Except the different material parameters for the drop phase and the bulk phase, the conservative equations above are valid for both phases. We define the nondimensional quantities as:

$$\begin{aligned} \bar{\mathbf{u}} &= \mathbf{u}/U, \quad \bar{\mathbf{x}} = \mathbf{x}/a, \quad \bar{t} = t/(a/U), \\ \bar{p} &= p/(\rho_b U^2), \quad \bar{T} = T/(|\nabla T_\infty|a), \quad \bar{\rho} = \rho/\rho_b, \quad (2) \\ \bar{\mu} &= \mu/\mu_b, \quad \bar{k} = k/k_b, \quad \bar{C}_p = C_p/C_{pb}, \\ \bar{\mathbf{F}}_\sigma &= \mathbf{F}_\sigma a/(\rho_1 U^2), \quad Re = Ua/\nu_b, \quad Ma = Ua/\kappa_b. \end{aligned}$$

Here, $\nu_b = \mu_b/\rho_b$ is the kinematic viscosity, and $\kappa_b = k_b/(\rho_b C_{pb})$ the thermal diffusivity of the matrix liquid. The nondimensional equations can be written as:

$$\nabla \cdot \bar{\mathbf{u}} = 0, \quad (3)$$

$$\begin{aligned} \frac{\partial(\bar{\rho}\bar{\mathbf{u}})}{\partial \bar{t}} + \nabla \cdot (\bar{\rho}\bar{\mathbf{u}}\bar{\mathbf{u}}) \\ = -\nabla \bar{p} + \frac{1}{Re} \nabla \cdot (\bar{\mu}(\nabla\bar{\mathbf{u}} + \nabla^T\bar{\mathbf{u}})) + \bar{\mathbf{F}}_\sigma, \quad (4) \end{aligned}$$

$$\bar{\rho}\bar{C}_p \left(\frac{\partial \bar{T}}{\partial \bar{t}} + \bar{\mathbf{u}} \cdot \nabla \bar{T} \right) = \frac{1}{Ma} \nabla \cdot (\bar{k}\nabla\bar{T}). \quad (5)$$

The boundary conditions for velocities are:

$$\begin{aligned} \bar{u}|_{\bar{x}=\bar{x}_0, \bar{x}_1} = \bar{v}|_{\bar{x}=\bar{x}_0, \bar{x}_1} = \bar{w}|_{\bar{x}=\bar{x}_0, \bar{x}_1} &= 0, \\ \bar{u}|_{\bar{y}=\bar{y}_0, \bar{y}_1} = \bar{v}|_{\bar{y}=\bar{y}_0, \bar{y}_1} = \bar{w}|_{\bar{y}=\bar{y}_0, \bar{y}_1} &= 0, \quad (6) \\ \bar{u}|_{\bar{z}=\bar{z}_0, \bar{z}_1} = \bar{v}|_{\bar{z}=\bar{z}_0, \bar{z}_1} = \bar{w}|_{\bar{z}=\bar{z}_0, \bar{z}_1} &= 0. \end{aligned}$$

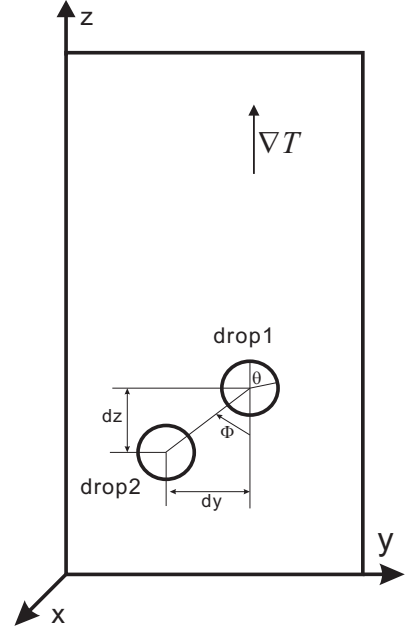


FIG. 1: The Sketch of two drops in the thermocapillary migration. Φ is the angle between the temperature gradient and the center line of two drops.

For energy equation, the *Dirichlet* boundary condition is adopted:

$$\begin{aligned} \bar{T}|_{\bar{x}=\bar{x}_0} = \bar{T}_0 + \bar{z}, \quad \bar{T}|_{\bar{x}=\bar{x}_1} = \bar{T}_0 + \bar{z}, \\ \bar{T}|_{\bar{y}=\bar{y}_0} = \bar{T}_0 + \bar{z}, \quad \bar{T}|_{\bar{y}=\bar{y}_1} = \bar{T}_0 + \bar{z}, \quad (7) \\ \bar{T}|_{\bar{z}=\bar{z}_0} = \bar{T}_0 + \bar{z}_0, \quad \bar{T}|_{\bar{z}=\bar{z}_1} = \bar{T}_0 + \bar{z}_1, \end{aligned}$$

The initial conditions are:

$$\begin{aligned} \bar{u}|_{\bar{t}=0} = \bar{v}|_{\bar{t}=0} = \bar{w}|_{\bar{t}=0} &= 0, \\ \bar{T}|_{\bar{t}=0} &= \bar{T}_0 + \bar{z}. \quad (8) \end{aligned}$$

In the following, symbols without overbars will be adopted to denote non-dimensional values.

II. NUMERICAL MODELS AND PARAMETERS

Fig. 1 indicates initial positions of two drops. The horizontal and vertical distances between two drops are dy and dz , respectively. The traditional definition of the non-dimensional distances are defined as $S_y = dy/2$ and $S_z = dz/2$ [7], and S_{y0} and S_{z0} denote the initial values of S_y and S_z . θ indicates the point on drop interface in the $x = 0$ plane: $\theta = 0$ is the front stagnation and $\theta = \pi$ or $\theta = -\pi$ the rear stagnation. Points in the clockwise direction from front stagnation are denoted with $\theta > 0$, otherwise, $\theta < 0$. In the full three dimensional model, the computation zone is set to be $6 \times 9 \times 24$

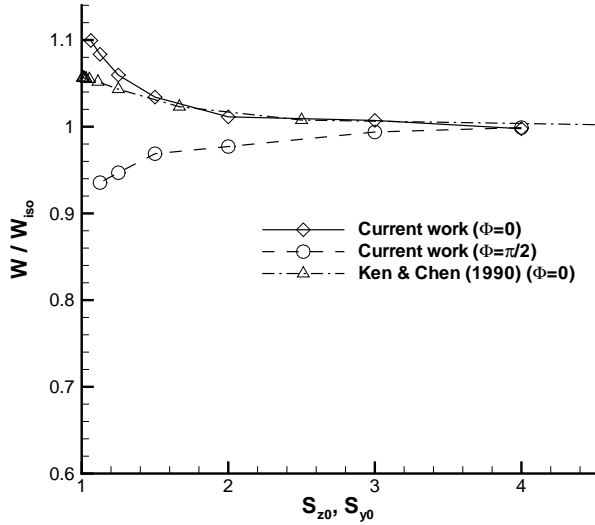


FIG. 2: The steady-state thermocapillary migration velocities of two drops with different initial distances. The horizontal ordinate is S_{z0} for $\Phi = 0$, and S_{y0} for $\Phi = \pi/2$. Here, $Re = Ma = 10^{-3}$.

on a grid of $60 \times 90 \times 240$. The time steps are 10^{-6} for $Re = Ma = 10^{-3}$, and 10^{-3} for other $Re \& Ma$ values. To save the computing time, the axisymmetric model is adopted in the cases of $\Phi = 0$ [22]. In axisymmetric simulations, drop1 in hotter region will be called the leading drop and drop2 in colder region the trailing drop, and S and S_0 are adopted to replace S_z and S_{z0} in the three-dimensional model. The computing domain is 6×24 with the resolution of 128×512 . The time steps are 5×10^{-7} for the simulations of $Re = Ma = 10^{-3}$ and 2×10^{-4} for all other $Re \& Ma$ values. In this paper, all material parameters of two drops are assumed to be the same.

Generally speaking, the non-dimensional thermocapillary migration velocities of drops are quite small (about 0.1), and the usually defined non-dimensional velocity (namely $\bar{\mathbf{u}} = \mathbf{u}/U_{max}$, where U_{max} is the maximum velocity in the flow field instead of $U = |\sigma_T| |\nabla T_\infty| a / \mu_b$) is even lower. The influence of the Re number in the current study is trivial and can be inferred from the results of the isolated drop. The role of the Re number will not be discussed here (simply set $Re = 1$ if not specified), and we will concentrate on the influences of thermal convection and initial distance.

To have a clear idea of the interaction of two thermocapillary drops, it is necessary to compare it with that of the isolated drop. In the following, the velocity of the isolated drop will be denoted as W_{iso} .

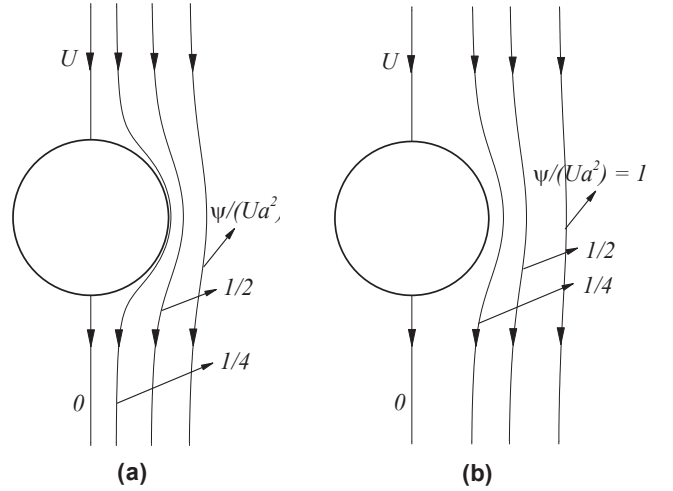


FIG. 3: Streamlines in a reference frame attached to the drop/sphere. (a) Potential flow, (b) Stokes flow.

III. THERMOCAPILLARY MIGRATION OF TWO DROPS WITH NEGLECTED INERTIA AND THERMAL CONVECTION

In this section, small Re and Ma numbers (10^{-3}) are adopted in simulations to compare with some previous analytical results. Fig. 2 shows the final migration velocities for $\Phi = 0$ & $\pi/2$. In the case of $\Phi = 0$, velocities of the two drops are very close, but faster than W_{iso} (see the solid line in Fig. 2). This phenomenon is also found in the previous analytical and numerical studies[7, 14]. In the case of $\Phi = \pi/2$, our three dimensional simulations show that the drop velocities in y or x direction are neglectable. The z direction velocities (W) of both drops are still the same, but they are slower than W_{iso} (the dash line in Fig. 2). In both cases, the increase of the initial drop distance makes the final drop velocity closer to W_{iso} .

Similarly, there are lots of researches on the interactions between two rigid spheres[15–17]. Using previous analytical linear results, we compare the difference between drops and rigid spheres. Assume the rigid sphere/drop has a constant velocity U , and the original point is in the center of the rigid sphere/drop. In the spherical coordinate (r, θ, ϕ) , the potential flow, which describes the thermocapillary motion of the drop, is written as[18]:

$$v_r = U \frac{a^3}{r^3} \cos \theta, \quad v_\theta = -\frac{1}{2} U \frac{a^3}{r^3} \sin \theta. \quad (9)$$

Here, $\theta = 0$ is the motion direction. The motion of the rigid sphere is described by the Stokes flow[19]:

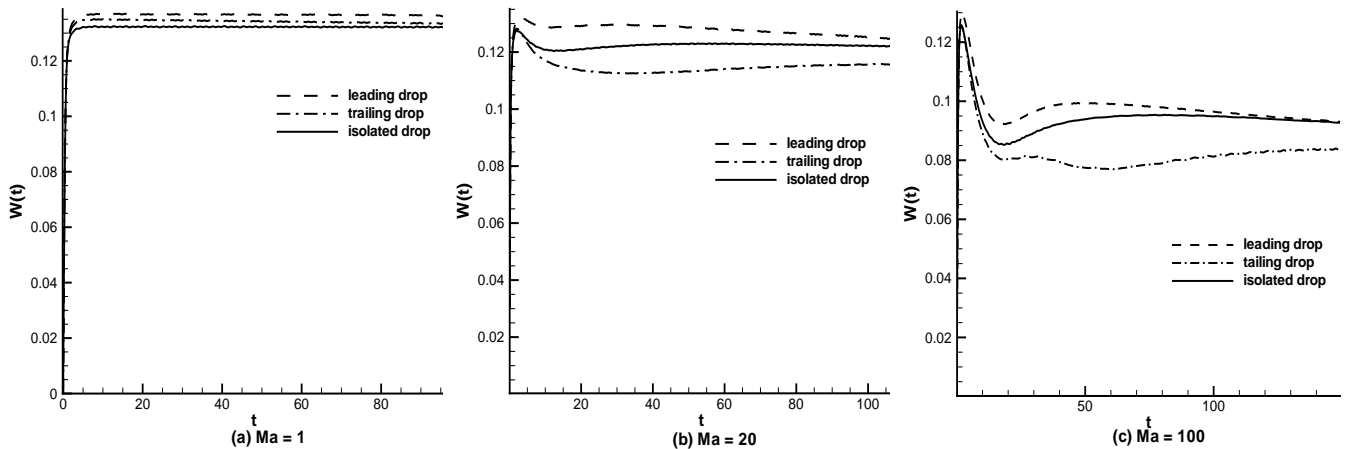


FIG. 4: The migration velocities of the leading drop, the trailing drop, and the isolated drop with $Re = 1$ and $S_0 = 1.5$.

IV. THERMOCAPILLARY MIGRATION OF TWO DROPS WITH FINITE INERTIA AND THERMAL CONVECTION

$$v_r(r, \theta) = \frac{1}{2}U\left(3\frac{a}{r} - \frac{a^3}{r^3}\right)\cos\theta$$

$$v_\theta(r, \theta) = -\frac{1}{4}U\left(3\frac{a}{r} + \frac{a^3}{r^3}\right)\sin\theta. \quad (10)$$

It is clear that, with the increase of r , the velocities for the rigid sphere and drop are decaying in the magnitude of $O(1/r^3)$ and $O(1/r)$, respectively. The velocity perturbation in potential flow spreads in a relatively small region (Fig. 3(a)), and has obvious directionality because the liquid in the front of the moving drop will be supplied to the back of the drop. For Stokes flow, the velocity perturbation spreads in a fairly large region, and the surrounding liquid tries to move with the sphere (Fig. 3(b)).

The drag coefficients of both rigid spheres are always lower than that of the isolated sphere [20, 21], which means two spheres will move faster than an isolated one. When the nonlinear effect is strong, the main interest in the interaction between rigid spheres is drag coefficients changed by the wake flow behind the leading body. However, in the thermocapillary study, the disturbed temperature field is the most important, and we will concentrate on it in the following section.

A. Influence of thermal convection for the cases of $\Phi = 0$

Firstly, we study the influence of the Ma number on the interaction between two droplets in thermocapillary motion with $S_0 = 1.5$ and $Re = 1$.

In the case of $Ma = 1$, the leading drop is faster than the trailing drop, but both of them move faster than the isolated drop (Fig. 4(a)). This is similar to what we have discussed in the last section. For $Ma = 20$, the leading drop is faster than the isolated drop throughout the simulation, while the speed of the trailing drop is up to 8% lower than W_{iso} (Fig. 4(b)). For $Ma = 100$, the trailing drop is even slower, and its velocity is up to 20% lower than W_{iso} (Fig. 4(c)).

Figs. 5 are the isotherms around the drops. When the Ma number is small, the isotherms around the drops are almost straight and evenly spaced throughout the simulation (Figs. 5(a)(d)). When the Ma number is increased, isotherms near $r = 0$ arch to the hotter region, and there is a closed cold zone arising in the droplet (Figs. 5(c)(f)). The temperature at the rear stagnation point of the leading drop is lower than that of the isolated drop, and the temperature gradient of the trailing drop is also reduced.

Fig. 6 shows the temperature difference between the point on drop surface and the front stagnation (to get a clear idea of this difference, the corresponding value of the isolated drop is subtracted in Figs. 6, 8 and 14). It can be seen that the temperature difference between the front and rear stagnation points of the leading drop

(solid line) is larger than that of the isolated drop; on the contrary, the difference for the trailing drop (dashed line) is smaller than that of the isolated drop, and will decrease with increasing Ma numbers. Fig. 6 clearly shows that the influence of the thermal convection on trailing drops is much stronger than that on leading drops.

When the heat convection is stronger, the influence on the trailing drop is also bigger. Hence, the separated distances ($S - S_0$) increase more rapidly for larger Ma numbers (Fig. 7). Note that the separating speed of $Ma = 100$ before $t = 60$ is lower than that of $Ma = 20$. This is because the fluctuation process of migrating speed in the beginning is longer for larger Ma number[2]. For example, the thermal wake left by leading drop with $Ma = 100$ is not fully developed until $t = 60$ (Fig. 5(c)(f)), and the velocity difference between leading and trailing drops is not so large.

Temperature differences for $Ma = 20$ at various moments are shown in Fig. 8. At $t = 20$, the temperature difference of the leading drop becomes bigger than that of isolated drop, and starts to become smaller afterwards. When the thermal convection effect and the temperature disturbance caused by the leading drop are fully developed, the temperature difference of the trailing drop reaches its minimum at $t = 40$, and starts to become larger afterwards.

B. Influence of initial distance for the cases of $\Phi = 0$

Obviously, there will be no interaction between drops if they are far enough from each other, so it is interesting to know the critical initial distance at which both droplets migrate like an isolated one.

Several different initial distances are tested for the case of $Re = 1$ and $Ma = 20$ (Figs. 9). The curve of the leading drop with $S_0 = 3$ is almost identical to that of the isolated drop (Fig. 9(a)), while the critical initial distance is 5 for the trailing drop (Fig. 9(b)). It seems that the thermal wake left by the leading drop affects the trailing drop at a longer distance than the distance at which the trailing drop interferes the leading drop.

When the Ma number is increased to 100, the critical initial distance for the leading drop remains to be $S_0 = 3$ (Fig. 10(a)). On the other hand, the thermal wake left by the leading drop is much longer and the critical initial distance for the trailing drop seems longer than 5.

Figs. 11 shows the time evolutions of distances between two drops. It's clear that the smaller the initial

distance between the two drops, the faster they will separate from each other. In the later stage of simulations, it seems that the distance differences caused by various initial distances vanish, and the final distance between drops (of course, if they are not too far away apart) is determined by other parameters.

C. Influence of thermal convection for the cases of $\Phi \neq 0$

In this subsection, the full three dimensional problem with $Re = 1$, $Ma = 20$ and $S_{y0} = S_{z0} = 1.35$ is studied. In this simulation, both drops have zero velocities in the x direction. In the vertical direction, the upper drop1 migrates slower than the isolated drop while the lower drop2 moves faster than the isolated drop (Fig. 12(a)). As a result, the vertical distance between the two drops is always decreasing (see the solid line in Fig. 15).

The isotherms at $t = 60$ are shown in Fig. 13. It can be seen that the thermal convection of the lower left drop2 causes the bending of isotherms around the upper right drop1. Compared with the isolated drop, the temperature gradient on the lower part of the left drop2 is reduced, while that on the upper part of the right drop1 is enlarged. In order to get a better understanding of the velocities in z direction (W), we study the temperature distributions at $t = 60$ in the $x = 0$ plane (Figs. 14). Compared with the isolated drop, the temperature difference between front and rear stagnation points of drop2 is larger, while that of drop1 is smaller.

The drop velocities in y direction (V) are plotted in Fig. 12 (b). It is found that drop1 is always trying to move away from drop2 in y direction. Drop2 moves towards drop1 in the beginning, but starts to move away since $t \approx 30$. Because V_{drop2} is always larger than V_{drop1} , the horizontal distance between two drops is increasing throughout the simulation.

D. Influence of the initial distance for the cases of $\Phi \neq 0$

In this subsection, three sets of simulations with $Re = 1$ and $Ma = 20$ starting from different initial distances are studied:

1. $(S_{y0}, S_{z0}) = (1.35, 1.35)$;
2. $(S_{y0}, S_{z0}) = (1.1, 1.35)$;

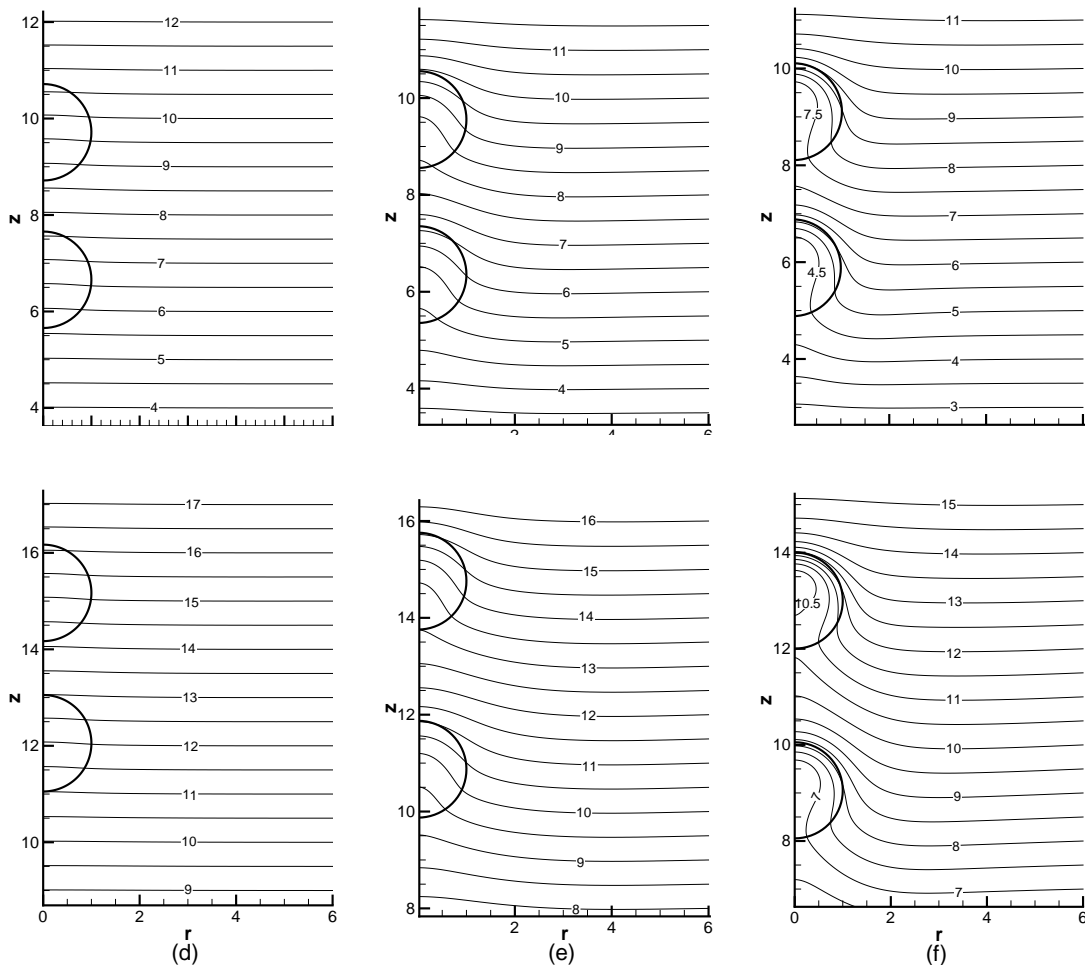


FIG. 5: The isotherms around the two droplets with $Re = 1$ and $S_0 = 1.5$. The first row is at $t = 20$, and the second row $t = 60$. The first column: $Ma = 1$; the second column: $Ma = 20$; the third column: $Ma = 100$.

3. $(S_{y0}, S_{z0}) = (1.35, 1.25)$.

It is clear that the smaller the initial horizontal distance, the larger the velocities of two drops in the y direction, and the bigger the temperature differences between the left and right sides of drops ($T(\theta) - T(-\theta)$, Fig. 16(b)).

With different Re and Ma numbers, the evolutions of distances between two drops for case1 are shown in Fig. 15. It can be seen that the two droplets separate very slowly when $Re = 1$ and $Ma = 1$. When the Re number is increased, the two drops get close faster in the vertical direction, while there are only trivial changes in separated distances for increasing Ma numbers.

Generally speaking, in the z direction, the lower drop2 moves faster than the isolated drop, while the upper drop1 moves slower than the isolated drop, and thus S_z is decreasing throughout any simulation in this subsection. If the simulation domain is big enough, drop2 would exceed drop1 in the z direction and slow down to a velocity

smaller than that of drop1. Then drop1 will start to catch up with drop2, and so on. Eventually, both droplets will reach a steady migration state when they are aligned horizontally, as indicated by Nas *et al.*[10, 11].

V. CONCLUSIONS

In this paper, the interactions of two nondeformable droplets in thermocapillary motion are studied. When the inertia and thermal convections are neglected, two vertically-placed drops will move faster than the isolated drop, while two horizontally-placed drops will move slower. For the finite Ma number and $\Phi = 0$, the leading drop moves faster than the isolated drop, while the trailing drop migrates slower than the isolated drop due to the disturbed temperature field left by the leading drop. When the two drops are closer, their interaction is stronger, but this intensive interaction will not last long

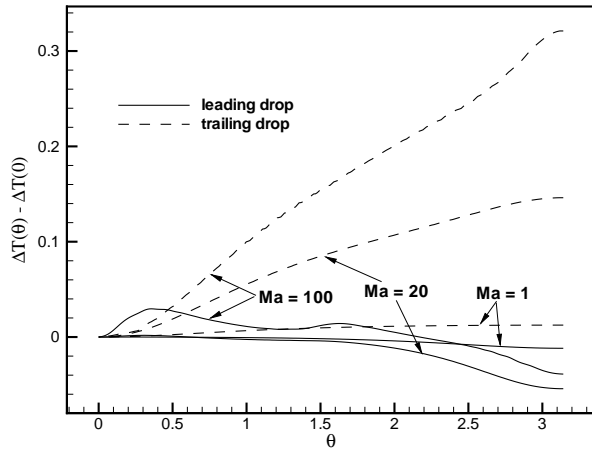


FIG. 6: Temperature difference between the point θ on in-

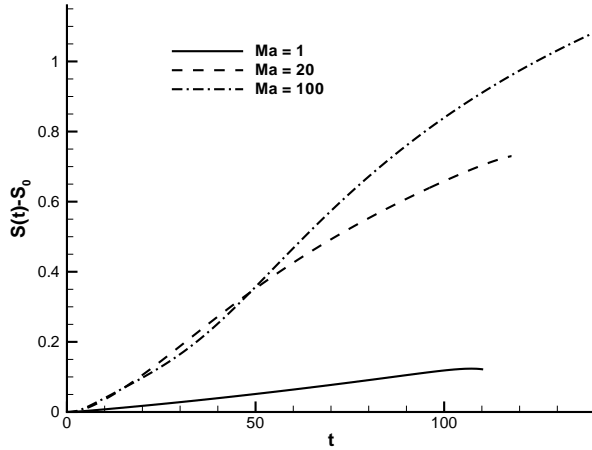


FIG. 7: Time evolutions of separation distances ($S - S_0$) between two drops for $Re = 1$ and $S_0 = 1.5$.

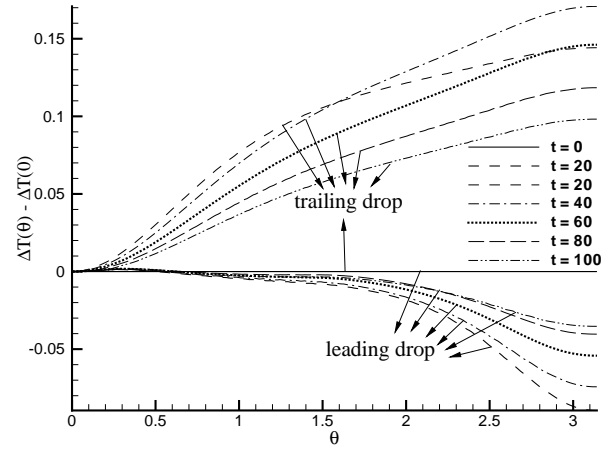


FIG. 8: The time evolution of the temperature difference for $Re = 1$, $Ma = 20$ and $S_0 = 1.5$.

because the velocity difference of two drops is also big. Once there is enough big gap between the two drops, they will migrate like the isolated drops. For the finite Ma number and $\Phi \neq 0$, the motions of two droplets are still limited in the $y - z$ plane. The upper drop1 migrates slower while the lower drop2 migrates faster than the isolated drop, which results in a smaller vertical distance and a bigger horizontal distance between the two drops. Tab. I sums up the velocities of drop1 and drop2 in the z direction (W_1, W_2) studied in this paper.

Here, we only explore a few interacting mechanisms of two droplets with a limited number of parameters. A wider range of parameters as well as deeper physical explanations should be included in the future works.

-
- [1] Young, N. O., Goldstein, J. S., and Block, M. J. The motion of bubbles in a vertical temperature gradient. *J Fluid Mech* **11**, 350-356 (1959)
 - [2] Yin, Z. H., Gao, P., Hu, W. R., and Chang, L. Thermocapillary migration of nondeformable drops. *Phys Fluids* **20**, 20082101 (2008)
 - [3] Meyyappan, M., Wilcos, W. R., and Subramanian, R. S. The slow axisymmetric motion of two bubbles in a thermal gradient. *J Colloid Interface Sci* **94**, 243-257 (1983)
 - [4] Meyyappan, M. and Subramanian, R. S. The thermocapillary motion of two bubbles oriented arbitrarily relative to a thermal gradient. *J Colloid Interface Sci* **97**, 291-294 (1984)
 - [5] Balasubramaniam, R. and Subramanian, R. S. Axisymmetric thermal wake interaction of two bubbles in a uniform temperature gradient at large Reynolds and Marangoni numbers. *Phys Fluids* **11**, 2856-2864 (1999)
 - [6] Anderson, J. L. Droplet interactions in thermocapillary motion. *Int J Multiphase Flow* **11**, 813-824 (1985)
 - [7] Keh, H. J. and Chen, S. H. The axisymmetric thermocapillary motion of two fluid droplets. *Int J Multiphase Flow* **16**, 515-527 (1990)
 - [8] Keh, H. J. and Chen, S. H. Droplet interactions in axisymmetric thermocapillary motion. *J Colloid Interface Sci* **151**, 1-16 (1992)
 - [9] Zhou, H. and Davis, R. H. Axisymmetric thermocapillary migration of two deformable viscous drops. *J Colloid Interface Sci* **181**, 60-72 (1996)
 - [10] Nas, S. and Tryggvason, G. Thermocapillary interaction of two bubbles or drops. *Int J Multi-phase Flow* **29**, 1117 -1135 (2003)
 - [11] Nas, S., Muradoglu, M., and Tryggvason, G. Pattern formation of drops in thermocapillary migration. *Int J Heat Mass Transfer* **49**, 2265-2276 (2006)
 - [12] Balasubramaniam, B., Lacy, C. E., Woniak, G., and Subramanian, R. S. Thermocapillary migration of bubbles and drops at moderate values of the Marangoni number in reduced gravity.

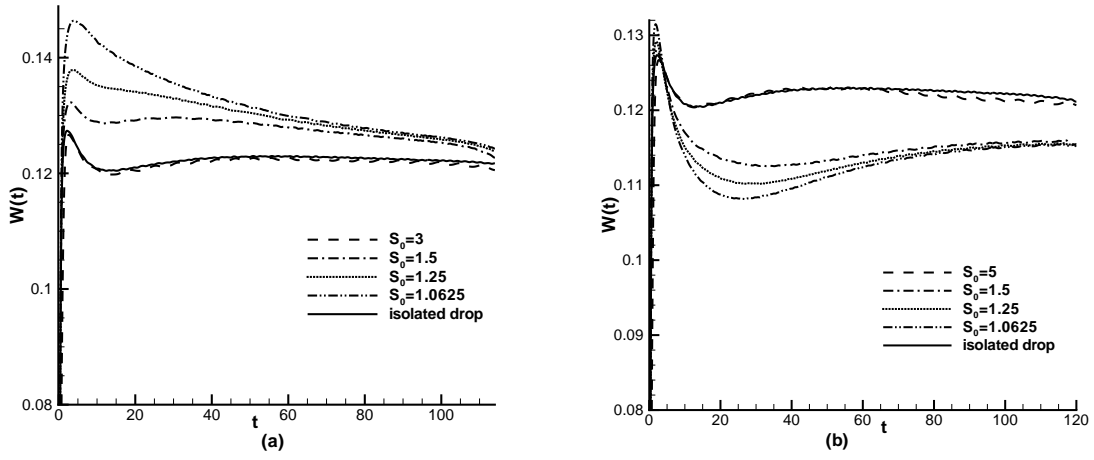


FIG. 9: Time evolutions of drop velocities for $Re = 1$ and $Ma = 20$ with various initial distances. (a) Leading drop, (b) trailing drop.

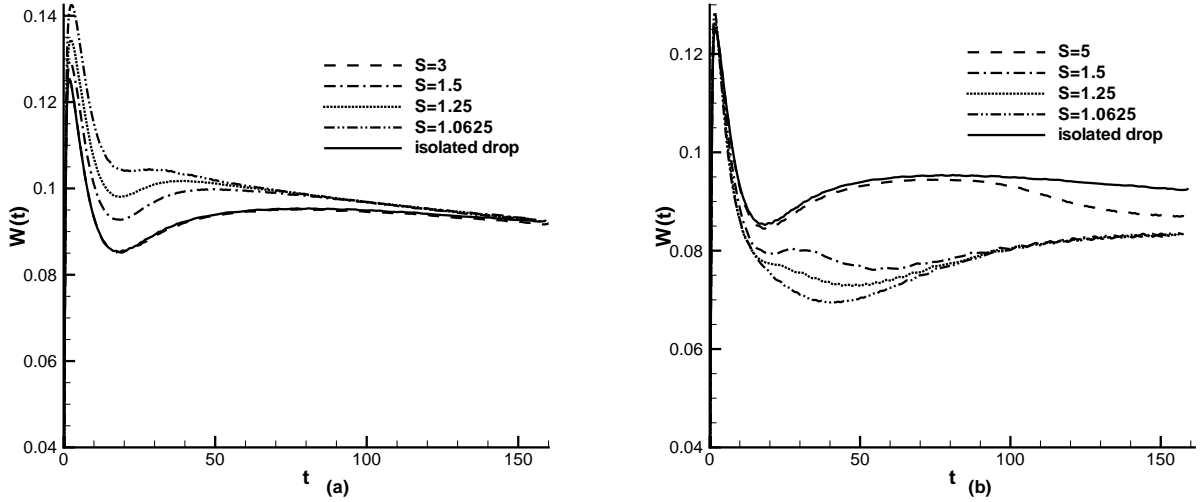


FIG. 10: $Re = 1$, $Ma = 100$, time evolutions of drop velocities with various initial distances. (a) Leading drop, (b) trailing drop.

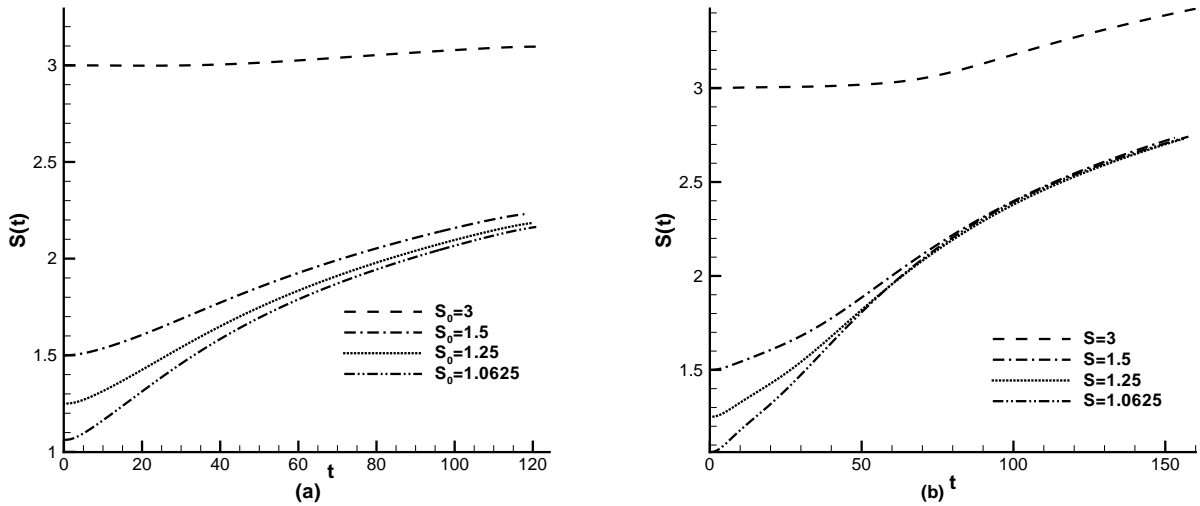


FIG. 11: Time evolutions of the separating distances between drops. (a) $Re = 1$, $Ma = 20$, (b) $Re = 1$, $Ma = 100$.

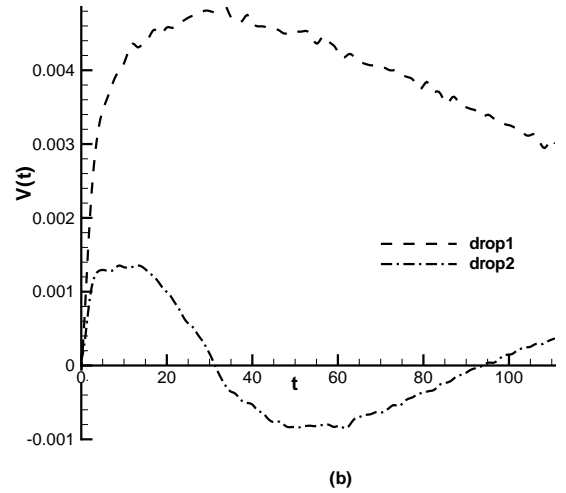
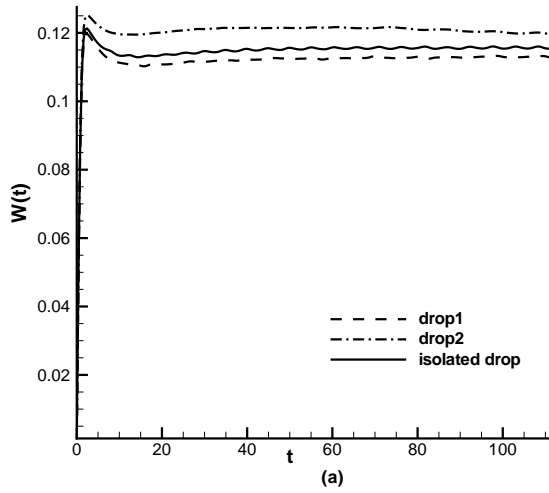


FIG. 12: $Re = 1$, $Ma = 20$ and $S_{y0} = S_{z0} = 1.35$, evolution of migration velocities, (a) velocity in z direction and (b) velocity in y direction.

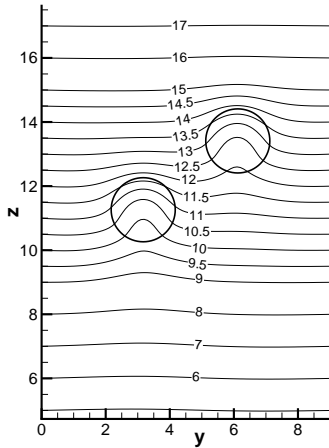


FIG. 13: Isotherms at $t = 60$. $Re = 1$, $Ma = 20$ and $S_{y0} = S_{z0} = 1.35$.

Phys Fluids **8**, 872-880 (1996)

- [13] Brady, P. T., Herrmann, M., and Lopez, J. M. Confined thermocapillary motion of a three-dimensional deformable drop. *Phys Fluids* **23**, 022101 (2011)
- [14] Gao, P. *Numerical Investigation of the drop thermocapillary migration* (in Chinese). Ph. D. dissertation, Chinese Academy

of Sciences, (2007)

- [15] Hick, W. M. On the motion of two spheres in a fluid. *Phil Trans Roy Soc* **171**, 455-492 (1880)
- [16] Herman, R. A. On the motion of two spheres in fluid. *Quart J Pure Appl Math* **22**, 204-262 (1887)
- [17] Kaneda, Y. and Ishii, K. The hydrodynamic interaction of two spheres moving in an unbounded fluid at small but finite Reynolds number. *J Fluid Mech* **124**, 209-217 (1982)
- [18] Batchelor, G. K. *An introduction to fluid mechanics*, Cambridge University Press, Cambridge, (1967).
- [19] Happel, J. and Brenner, H. *Low Reynolds number hydrodynamics*, Martinus Nijhoff Publishers, The Hague, 1965(1 ed.), 1973, 1983(reprint)
- [20] Stimson, M. and Jeffery, G. B. The motion of two spheres in a viscous fluid. *Proc Roy Soc A***111**, 110 (1926)
- [21] Goldman, A. J., Cox, R. G., and Brenner, H. The slow motion of two identical arbitrarily oriented spheres through a viscous fluid. *Chem Eng Sci* **21**, 1151-1170 (1966)
- [22] It has been realized that some nonaxisymmetrical behaviors might arise for the isolated drop when the full three-dimensional simulating domain is fairly small[13]. In this paper, we adopt a fairly large domain, and assume the nonaxisymmetrical effect can be neglected for moderate parameters.

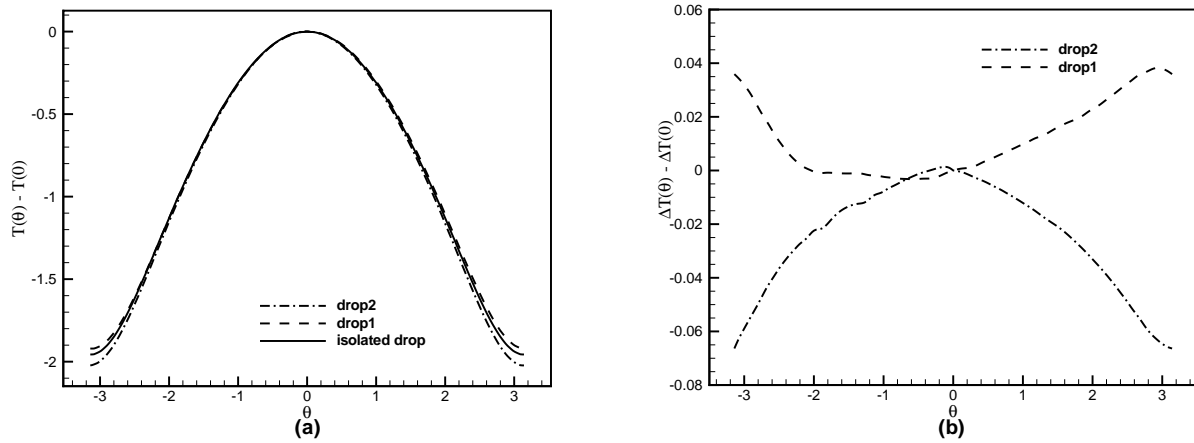


FIG. 14: The temperature distributing on the surface of drops in the $x = 0$ plane at $t = 60$. $Re = 1$, $Ma = 20$, $S_{y0} = S_{z0} = 1.35$ and $\Delta T(\theta) = T(\theta) - T_{iso}(\theta)$.

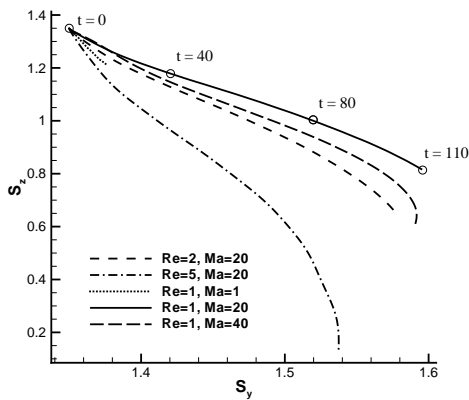


FIG. 15: The time evolution of the vertical and horizontal distances between two drops with $S_{y0} = S_{z0} = 1.35$.

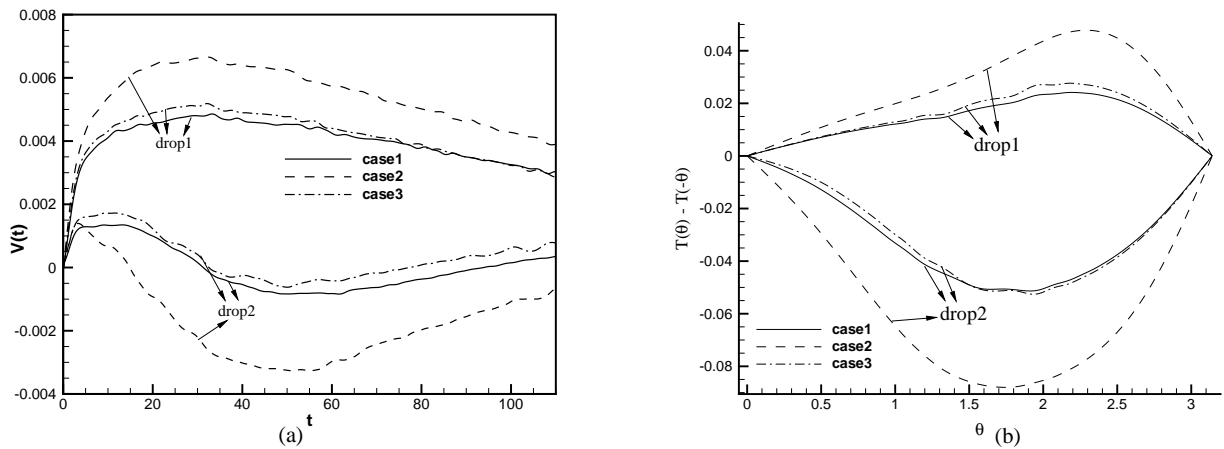


FIG. 16: (a) Time evolutions of the vertical velocities of the drops with various initial distances, (b) the temperature differences between the left and right sides of the drops.

Parameters	$Re = Ma = 10^{-3}$	$Ma = 1, RE = 1$	$Ma = 20, RE = 1$	$Ma = 100, RE = 1$	rigid Spheres
$\Phi = 0$	W_{1+}, W_{2+}	W_{1+}, W_{2+}	W_{1+}, W_{2-}	W_{1+}, W_{2-}	W_{1+}, W_{2+}
$\Phi = 0.68, \pi/4, 0.82$	—	—	W_{1-}, W_{2+}	—	W_{1+}, W_{2+}
$\Phi = \pi/2$	W_{1-}, W_{2-}	—	—	—	W_{1+}, W_{2+}

TABLE I: The velocities of drop1 (W_1) and drop2 (W_2) are compared with W_{iso} . ‘+’/‘-’ means the velocity is bigger/smaller than W_{iso} . The velocities of rigid spheres in Stokes flow are listed in the last row, the bigger/smaller velocity stands for the smaller/bigger resistance than that on the isolated rigid sphere.